ISIJ International, Vol. 41 (2001), No. 7, pp. 774–781

Improved Model for Static Recrystallization Kinetics of Hot Deformed Austenite in Low Alloy and Nb/V Microalloyed Steels

S. F. MEDINA and A. QUISPE

National Centre for Metallurgical Research (CENIM-CSIC), Av. Gregorio del Amo, 8, 28040-Madrid, Spain.
E-mail: smedina@cenim.csic.es

(*Received on November 20, 2000; accepted in final form on March 28, 2001*)

Using torsion tests a improved model has been constructed to predict the static recrystallization kinetics of deformed austenite in low alloy and microalloyed steels. The model quantifies the influence of the most common elements (C, Si, Mn, Mo) in low alloy steels and the typical elements (V, Nb) in microalloyed steels, when they are in solution. Activation energy (Q) is the parameter sensitive to the content and nature of each alloying element, and an expression for Q is shown as a function of the percentage of each one. Nb is the element that contributes most to increasing the value of Q, and thus that which most delays recrystallization kinetics. C is seen to be the only alloying element that contributes to lowering the value of Q, and thus to accelerating recrystallization kinetics. Extrapolation of the expression of Q to pure iron in the austenitic phase gives a value of 148 637 J mol^{-1}, which is similar to other values found in the literature for the grain boundary self-diffusion energy of pure Fe_γ. Static recrystallization kinetics follow Avrami's law and expressions are given for the parameter $t_{0.5}$ and the exponent n.

KEY WORDS: austenite; static recrystallization; low alloy steels; microalloyed steels.

1. Introduction

Though the static recrystallization of austenite started to be studied in the 1970's, the first expressions quantifying the influence of the different variables that intervene in hot deformation (strain, strain rate, temperature and grain size) on static recrystallization kinetics appeared in 1980. The model published by Sellars[1] supposed an important reference for better understanding the role of these variables, and opened up the possibility of modelling the phenomenon of static recrystallization and predicting the evolution of microstructures in hot rolling. Most models have been published since 1990 and a large number of them have been based on expressions similar to that of Sellars, changing the quantitative influence of the different variables from one model to another.

Most of the published models for predicting the static recrystallization of austenite[1–11] have not taken into account the influence of the content of each alloying element, and only some take into account the influence of certain elements. In general, authors establish a single model for C–Mn type steels, irrespective of their chemical composition, and another for Nb microalloyed steels, irrespective of the Nb content. However, alloying elements certainly exert an influence on static recrystallization, and though the first studies undertaken in this respect only dealt with their qualitative influence,[12,13] Medina and Mancilla published a model that established the quantitative influence of some alloying elements (Si, Mn, Mo, Nb, Ti).[14,15] This influence was quantified by means of an expression for activation energy (Q), though this expression unfortunately reveals very little about the atomic mechanisms that occur during recrystallization. This is because of the dual character of a nucleation and growth reaction. The rate at which a metal recrystallizes depends on the rate at which nuclei form, and on the rate at which they grow. These two rates also determine the final grain size of a recrystallized metal.

The variation in activation energy according to the chemical composition showed that solute atoms interact with the grain boundaries. If the size of a foreign atom and the parent crystal are different, then there will be an elastic stress field introduced into the lattice by each foreign atom. The elements that most distort the lattice structure of austenite have the largest effect on grain boundary migration. The greater the atomic volume of the substitutional elements, the greater the distortion.[16]

The intention of this work has been to perfect the aforementioned model,[14,15] substantially increasing the number of steels used up to a total of twenty-six. In this way it is aimed to give the model a more universal character, and as the same time to achieve greater precision in determining the quantitative influence of the different alloying elements, including C and V in addition to those mentioned above. Thus recrystallization kinetics are modelled at temperatures in the austenitic phase and where the elements are in solution. The influence of grain size, strain and strain rate have also been studied.

2. Materials and Experimental Procedure

The steels were manufactured by electroslag remelting in a laboratory unit capable of producing 30 kg ingots. Their

Table 1. Chemical composition (wt%), cooling critical temperatures (Ar_3, at 0.2 K/s) and austenite grain size (D) at reheating temperature (RT), being X_i=Mo, V, Nb.

Steel	C	Si	Mn	X_i	N	Ar_3, °C	RT, °C	D,μm
C1	0.15	0.21	0.74	-	-	810	1230	187
C2	0.36	0.20	0.82	-	-	740	1230	189
C3	0.53	0.21	0.71	-	-	714	1230	179
S1	0.11	0.26	0.55	-	-	814	1230	143
S2	0.11	1.65	0.47	-	-	896	1230	104
M1	0.11	0.26	0.68	-	-	835	1230	212
M3	0.11	0.25	1.55	-	-	772	1230	192
Mo1	0.44	0.24	0.79	Mo=0.26		704	1230	180
Mo2	0.44	0.23	0.79	Mo=0.38	-	714	1230	205
Mo3	0.42	0.27	0.79	Mo=0.18	-	709	1230	193
							1100	137
							1000	83
V1	0.11	0.24	1.10	V=0.043	0.0105	786	1230	172
V2	0.12	0.24	1.10	V=0.060	0.0123	782	1230	167
V3	0.11	0.24	1.00	V=0.093	0.0144	784	1100	125
							1230	165
V4	0.21	0.20	1.10	V=0.062	0.0134	768	1100	95
							1200	180
V5	0.33	0.22	1.24	V=0.076	0.0146	716	1200	165
V6	0.35	0.21	1.23	V=0.033	0.0121	715	1200	170
V7	0.42	0.24	1.32	V=0.075	0.0200	718	1200	162
V8	0.37	0.24	1.42	V=0.120	0.0190	721	1200	157
N1	0.11	0.24	1.23	Nb=0.041	0.0112	786	1230	122
N2	0.11	0.24	1.32	Nb=0.093	0.0119	786	1230	116
N3	0.21	0.18	1.08	Nb=0.024	0.0058	768	1250	210
N4	0.21	0.19	1.14	Nb=0.058	0.0061	769	1250	190
N5	0.51	0.25	1.20	Nb=0.026	0.0105	674	1280	430
N7	0.29	0.22	1.30	Nb=0.066	0.0062	751	1295	415
N8	0.20	0.20	1.0	Nb=0.007	0.0056	770	1250	140
N9	0.46	0.24	1.25	Nb=0.009	0.010	704	1250	190

compositions are shown in **Table 1**. The twenty-six steels include different combinations of C, N and metallic precipitate-forming elements such as V and Nb. Given that the nitrides, carbides or carbonitrides of Nb are less soluble in austenite than those of V, the limit imposed on C and N contents has been that the solubility temperature should not exceed 1 300°C. In this sense, some compositions, such as steel N9, with a very low Nb content and high C content, are not currently standard compositions, but the interest in studying them lies in ascertaining the influence of low Nb contents on recrystallization.

Torsion specimens were prepared with a gauge length of 50 and 6 mm diameter. The reheating temperature prior to torsion deformation was different depending on whether the steel was microalloyed with V or with Nb (Table 1), as the solubility temperature of the precipitates depends on their nature and on the precipitate-forming element content. For steels containing vanadium, designated by the letter V, the reheating temperature was 1 230°C for steels V1, V2 and V3 and 1 200°C for the rest, which is sufficient to dissolve vanadium nitrides and carbides. In the case of niobium steels, designated by the letter N, the reheating temperature depended on the C, Nb and N contents, but was always above the solubility temperature of niobium carbonitrides.[17]

All the C–Mn/Si steels (C1, C2, C3, M1, M2, S1, S2), C–Mo steels (Mo1, Mo2) and the microalloyed steels V1, V2, V3, N1 and N2 have been studied previously[14,15] in relation with static recrystallization, but their results are taken into account in order to achieve greater universalization of the model proposed in this work.

To ensure that the testing temperatures corresponded to the austenitic phase, critical transformation temperatures were measured by dilatometry at a cooling rate of 0.2°C/s (Table 1). Once the specimens had been reheated the temperature was rapidly lowered to the testing temperature, where it was held for a time of no more than 1 min in order to prevent precipitation taking place before the strain was applied. The testing temperatures varied between 1 100°C and 800°C for V steels and between 1 150°C and 850°C for Nb steels. In all cases, the testing temperatures were fixed as the recrystallized fraction was determined and the recrystallized fraction curves drawn, so that the curves finally obtained would include curves where strain induced precipitation had taken place and curves where it had not, as will be seen below.

The magnitudes of torsion (torque, no. of revolutions) and the equivalent magnitudes (stress, strain) have been related according to Von Mises criterion.[18] Most of the steels used were tested at strains of 0.20 and 0.35, respectively,

and at a constant strain rate of $3.63\,s^{-1}$ ($=1000$ rev/min). The strain of 0.35 in no case exceeded the peak strain necessary for dynamic recrystallization to commence in any of the steels.

Other tests at different strain rates (0.54, 1.45, $5.08\,s^{-1}$) and different reheating temperatures (1 230, 1 100, 1 000°C) were carried out in order to quantify the influence of the strain rate and grain size, respectively.

Using the "back extrapolation" method,[19,20] the recrystallized fraction (X_a) after an interval of hot working was calculated from the expression:

$$X_a = \frac{\sigma_m - \sigma_r}{\sigma_m - \sigma_0} \quad \text{.....(1)}$$

where σ_m is the flow stress immediately before unloading and σ_0 and σ_r are the initial flow stress recorded during prestraining and the stress corresponding to the intersection of the reloading line with the line obtained by superimposing the prestraining curve on the reloading curve. With this method the softened fraction is approximately equal to the recrystallized fraction. In other words, the effect of recovery is excluded from the double compression data.[21]

3. Static Recrystallization Kinetics Expressions

The static recrystallization kinetics of austenite can be described by an Avrami equation in the following way:[4]

$$X_a = 1 - \exp\left[-0.693\left(\frac{t}{t_{0.5}}\right)^n\right] \quad \text{.....(2)}$$

where X_a is the fraction of the recrystallized volume and $t_{0.5}$ is the time corresponding to half of the recrystallized volume, which depends practically on all the variables that intervene in hot deformation and whose most general expression follows a law of the type:

$$t_{0.5} = A\varepsilon^p \dot{\varepsilon}^q D^s \exp\frac{Q}{RT} \quad \text{.....(3)}$$

where ε is the strain, $\dot{\varepsilon}$ the strain rate, D the grain size, Q the activation energy, T the absolute temperature, $R=8.3145\,J\,mol^{-1}\,K^{-1}$, and p, q and s are parameters. Thus, the construction of the model will be based on the determination of the magnitudes: A, Q, p, q, s and n.

4. Results

Given the high number of steels tested, it was necessary to establish some working hypotheses in order to simplify the number of tests to be carried out. These hypotheses have been checked with other models already published, as mentioned above, and are as follows:

(a) Temperature and strain are the magnitudes that have the greatest influence on recrystallization. Thus, the recrystallization kinetics of each steel will be studied at different temperatures and at least two strains.

(b) Grain boundaries are preferential sites for the nucleation of new recrystallized grains and their function is the same in all the steels studied, whatever their composition. Thus, the influence of grain size will be studied in two steels (Mo3, V4), generalizing the results to the rest.

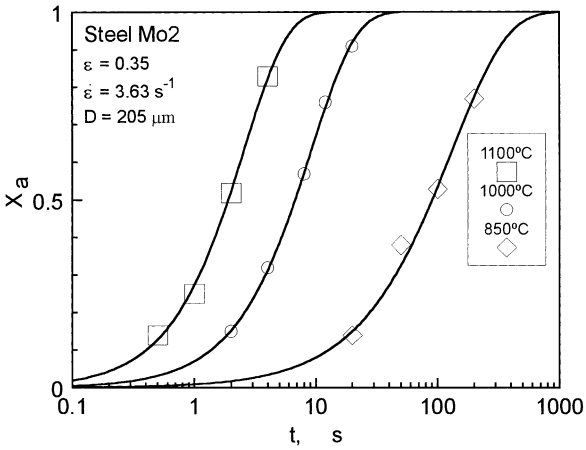

Fig. 1. Recrystallized fraction (X_a) plotted against time (t). Steel Mo2; $\varepsilon=0.35$.

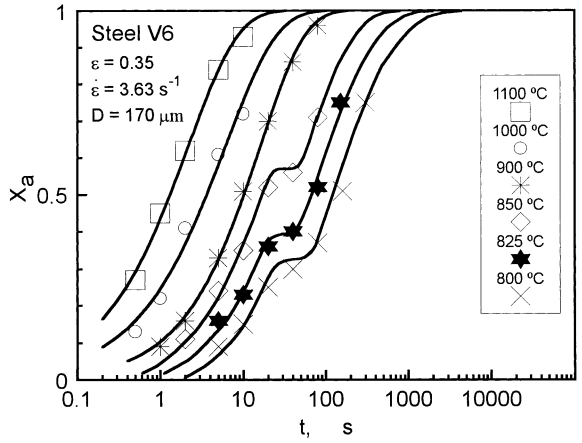

Fig. 2. Recrystallized fraction (X_a) plotted against time (t). Steel V6; $\varepsilon=0.35$.

(c) Strain rate is the variable with the smallest influence on recrystallization kinetics, to the point that many authors underestimate its effect.[5] An increase in the strain rate implies an increase in the density of dislocations, but these are not preferential sites for nucleation like the grain boundaries, and thus this variable is less important than the grain size. Therefore, the influence of strain rate will also be studied in four steels (C3, V7, N5) and the results generalized to the others.

The recrystallized fraction (X_a) was determined against time (t) for all twenty-six steels, at the temperatures and strains indicated above. **Figure 1** shows X_a for steel Mo2, in the conditions indicated in the graph, and represents an example of SRK for non-microalloyed steels where all the curves follow Avrami's law, whatever the deformation temperature in the austenitic phase. **Figure 2** shows X_a for one of the V microalloyed steels, where a plateau can be seen to form after a certain temperature. This plateau is a consequence of strain-induced precipitation. The same occurs in Nb microalloyed steels (**Fig. 3**) where the plateau is similar, though here it starts to form at higher temperatures than in the previous case, due to the fact that the precipitates of Nb,

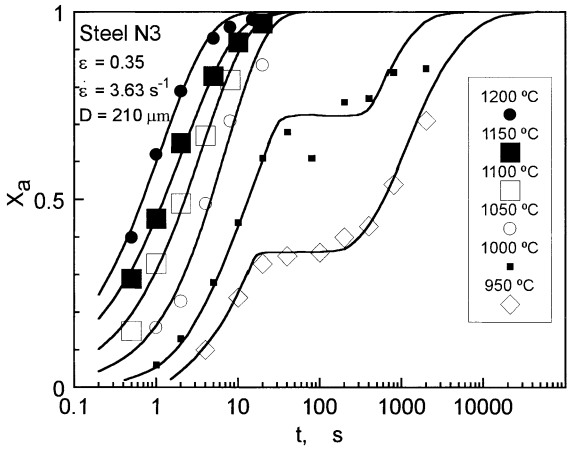

Fig. 3. Recrystallized fraction (X_a) plotted against time (t). Steel N3; ε=0.35.

nitrides, carbides or carbonitrides, are less soluble in austenite than the precipitates of V.[17] In both groups of steels, once the plateau has finalized, the recrystallized fraction continues to progress until it reaches 100%.

The plateau starts to appear below a certain temperature known as the Static Recrystallization Critical Temperature (SRCT). In other words, SRCT represents the temperature below which induced precipitation starts and depends on all the variables that intervene in hot deformation, including the chemical composition of the steel. The methodology for its determination and its modelling as a function of these variables have been reported elsewhere.[22,23] Technically, SRCT represents the lowest temperature at which all the microalloying elements are in solution.

According to Eq. (2), by regression of the experimental points, the values of $t_{0.5}$ and of n were determined on each X_a curve against t for all the C–Mn/Si/Mo steels. In the case of microalloyed steels, $t_{0.5}$ and n were determined only on those curves that do not present a plateau, *i.e.* for temperatures above SRCT. $t_{0.5}$ was also determined on some curves where the plateau appeared for recrystallized fractions of more than 50%, since in these cases the section of the curve prior to the plateau could be assumed to be an X_a curve where the microalloying elements are practically in solution.

All the values of $t_{0.5}$ and n thus determined are shown in **Tables 2–4**, each respectively referring to one group of steels: a first group for non-microalloyed steels (Table 2), a second group for V microalloyed steels (Table 3) and a third group for Nb microalloyed steels (Table 4). These values have been taken to construct the model proposed in this work, which is developed in the following section.

5. Discussion and Improved Model

According to Eq. (3), Q was measured taking $\ln(t_{0.5})$ as a function of $1/T$, the slope being equal to Q/R. While the graphic representation for low alloy steels (**Fig. 5**) is a straight line, the plots for microalloyed steels show two different parts (**Figs. 6–7**), it being possible to observe the two stages corresponding to temperatures above and below SRCT, respectively. The step from one stage to another indicates a discontinuity not only of the derived function but also of the function itself $\ln t_{0.5}(1/T)$. In other words, the value of activation energy changes from one stage to another and this occurs at a constant temperature during the time that precipitation takes place. After precipitation the activation energy increases significantly, which obviously results in greater difficulty for the austenite to recrystallize.

Table 2. Experimental values of $t_{0.5}$ and n for low alloy steels.

Steel	Temperature (°C)	ε=0.20		ε=0.35	
		$t_{0.5}$	n	$t_{0.5}$	n
C1	1100	2.97	1.02	1.08	0.62
	1000	7.03	0.84	2.81	0.71
	850	63.68	0.69	28.04	0.78
C2	1100	1.98	1.34	0.88	0.99
	1000	5.67	1.26	2.26	0.83
	850	60.22	0.96	24.90	1.00
C3 $\dot{\varepsilon}=0.54s^{-1}$	1000	12.27	0.71	-	-
C3 $\dot{\varepsilon}=1.45s^{-1}$	1000	7.82	0.72	-	-
C3 $\dot{\varepsilon}=3.63s^{-1}$	1100	1.93	1.22	0.82	1.02
	1000	4.47	1.02	1.55	1.08
	850	43.09	0.95	14.36	0.97
C3 $\dot{\varepsilon}=5.08s^{-1}$	1000	3.86	1.03	-	-
M1	1100	4.15	1.32	0.92	0.64
	1000	11.33	0.99	2.87	0.79
	900	46.85	0.81	13.92	0.67
M3	1100	3.80	0.91	1.13	0.70
	1000	14.55	0.90	3.98	0.71
	850	163.27	0.93	40.92	0.69
S1	1100	2.45	1.44	0.94	1.19
	1000	8.13	1.15	2.51	1.14
	900	30.65	1.20	11.06	1.12
S2	1150	1.47	0.91	-	-
	1100	3.21	0.83	1.26	1.09
	1075	4.3	0.7	2.17	0.87
	1000	19.78	0.73	6.17	0.62
Mo1	1100	4.00	1.43	1.30	1.07
	1000	12.34	1.32	4.04	1.25
	850	133.75	1.14	52.25	1.04
Mo2	1100	5.05	1.50	1.89	1.21
	1000	15.59	1.29	6.73	1.18
	850	216.25	0.98	90.23	0.96
Mo3 D=193μm	1100	3.50	1.29	1.43	1.17
	1000	8.31	1.36	3.57	1.16
	850	75.53	1.13	38.66	1.24
Mo3 D=137μm	1000	-	-	2.47	1.07
Mo3 D=83μm	1000	-	-	1.54	0.92

The experimentally determined values of Q for all the steels, and for microalloyed steels only in the stage where all elements are in solution, are given in **Table 5**. In the table it can be seen that each steel shows a different value, thus indicating that chemical composition, as well as the variation in the content of each alloying element, has an influence on SRK. The values of Q found are lower than those reported by other authors,[7–10] both for low alloy steels and for microalloyed steels. This is most likely due to the fact that the back extrapolation method only determines the recrystallized fraction, thus excluding the fraction softened due to recovery.

The specific influence of each alloying element has been reported elsewhere,[14] except for C and V. The influence of Si was studied comparing the Q values for steels S1 and S2. Similarly the influence of the Mn content was studied with

Table 3. Experimental values of $t_{0.5}$ and n for V microalloyed steels.

Steel	Temperature (°C)	ε=0.20		ε=0.35	
		$t_{0.5}$(s)	n	$t_{0.5}$(s)	n
V1	1100	3.47	0.91	1.06	0.70
	1000	11.57	0.81	3.52	0.86
	900	50*	-	12.57	0.87
	850	-	-	32*	-
V2	1100	2.65	1.16	0.84	0.65
	1000	7.19	0.98	2.64	0.79
	900	32*	-	12*	-
	875	-	-	20*	-
V3 D=165μm	1100	2.41	1.26	0.81	0.83
	1000	7.03	1.18	2.47	0.81
	950	-	-	7*	-
V3 D=125μm	1100	1.80	0.98	-	-
	1000	6.78	0.88	-	-
	950	20*	-	-	-
V4	1100	-	-	0.76	0.583
D=180μm	1000	-	-	2.60	0.608
	900	-	-	9.80	
V4	1000	-	-	1.27	0.741*
D= 95μm	900	-	-	4.43	0.679*
	850	-	-	11*	
V5	1100	2.40	1.03	1.31	0.77
	1000	7.08	1.02	3.56	0.80
	950	-	-	6.80	0.77
	900	24*	-	14.40*	-
V6	1100	3.42	1.03	1.31	0.72
	1000	9.09	0.88	3.61	0.70
	900	29.97	0.83	10.17	0.79
	850	-	-	19.20*	-
V7 $\dot{\varepsilon}=3.63s^{-1}$	1100	-	-	0.93	0.70
	1000	-	-	2.35	0.78
	950	-	-	3.97	0.84
	900	-	-	8*	-
V7 $\dot{\varepsilon}=0.91\ s^{-1}$	1100	-	-	2.26	0.62
	1000	-	-	6.01	0.59
	950	-	-	11.44	0.56
	900	-	-	19*	-
V8	1100	3.23	0.86	1.24	0.77
	1000	8.25	0.844	3.30	0.83
	975	12.53	0.797	-	-
	925	19.68*	-	6.23*	-
	900	-	-	9.50*	-

* Values for temperatures below SRCT

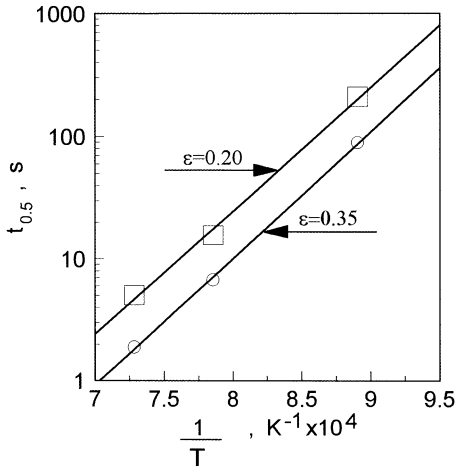

Fig. 4. Plot of $t_{0.5}$ against the reciprocal of the absolute temperature. Steel Mo2.

steels M1 and M3 and the influence of Mo with steels Mo1, Mo2 and Mo3. The influence of the V content, which was first studied with steels V1, V2 and V3,[14] has now been

Table 4. Experimental values of $t_{0.5}$ and n for Nb microalloyed steels.

Steel	Temperature (°C)	$\varepsilon=0.2$		$\varepsilon=0.35$	
		$t_{0.5}$ (s)	n	$t_{0.5}$ (s)	n
N1	1150	2.46	0.94	-	-
	1100	5.74	0.83	1.88	0.80
	1050	14.85	0.69	4.65	0.69
	1025	30*	-	-	-
	1000	-	-	13*	-
N2	1150	1.92	0.87	-	-
	1100	5.10	0.87	1.74	0.89
	1050	12*	-	3.78	0.69
	1025	-	-	10*	-
N3	1200	-	-	0.69	0.73
	1150	1.71	0.74	1.23	0.68
	1100	-	-	2.24	0.77
	1050	7.15	0.80	4.64	0.88
	1000	20*	-	12*	-
N4	1200	1.44	0.97	0.72	0.852
	1150	-	-	1.31	0.892
	1100	5.09	1.055	2.72	0.891
	1050	11*	-	6.1*	-
	1025	-	-	10.1*	-
N5 $\dot{\varepsilon}=3.63s^{-1}$	1200	-	-	1.14	1.38
	1150	-	-	1.63	1.40
	1100	-	-	2.51	1.36
	1050	-	-	4.04	1.33
N5 $\dot{\varepsilon}=1.09s^{-1}$	1200	-	-	2.45	1.07
	1150	-	-	3.94	1.08
	1100	-	-	6.26	1.14
N7	1200	2.62	0.98	0.86	0.943
	1150	5.33	1.05	1.80	0.888
	1050	-	-	8*	-
N8	1100	3.99	0.81	1.05	0.63
	1000	15.66	0.70	4.12	0.66
	950	47*	-	12.5*	-
	900	-	-	26*	-
N9	1100	3.51	0.84	1.30	0.680
	1000	10.07	0.72	4.27	0.696
	975	16.70*	-	-	-
	950	30*	-	10*	-

* Values for temperatures below SRCT

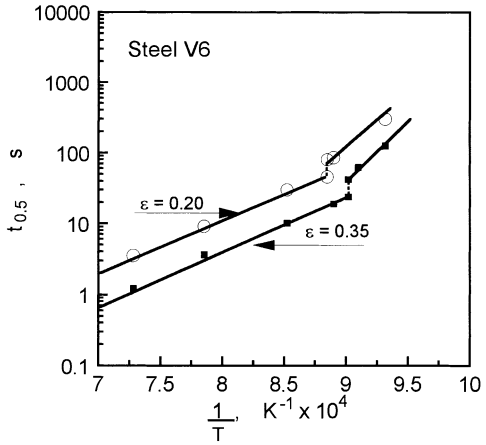

Fig. 5. Plot of $t_{0.5}$ against the reciprocal of the absolute temperature. Steel V6.

completed by comparing the Q values for the new V microalloyed steels V5, V6 and V8, which have approximately the same content of the other elements. Similarly, the influence of the Nb content has now been more amply studied with the new microalloyed steels, in addition to steels N1 and N2. The variation in the C content of many of the microalloyed steels has permitted a better evaluation of this element, since it was seen when comparing microalloyed steels with the same microalloying element content and na-

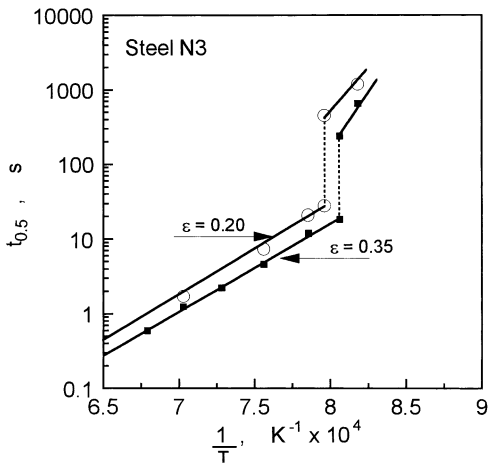

Fig. 6. Plot of $t_{0.5}$ against the reciprocal of the absolute temperature. Steel N3.

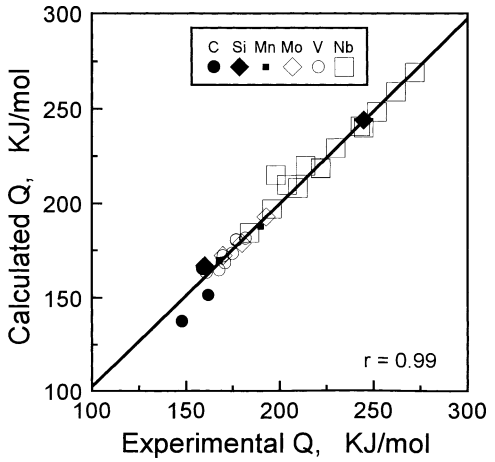

Fig. 7. Experimental activation energy (Q_e) *vs.* calculated activation energy (Q_c) for steels used.

ture but different C contents, that the latter contributed to slightly lowering the value of Q. In the regression calculations, both linear regression and power regression were used, adopting for each element the one with the least error. In this way the following expression was found for activation energy:

$$Q\,(\mathrm{J\cdot mol^{-1}}) = 148\,636.8 - 71\,981.3[\mathrm{C}] + 56\,537.6[\mathrm{Si}] + 21\,180[\mathrm{Mn}] + 121\,243.3[\mathrm{Mo}] + 64\,469.6[\mathrm{V}] + 109\,731.9[\mathrm{Nb}]^{0.15} \quad \text{.....(4)}$$

where each square bracket indicates the percentage by weight of the element indicated. It should be noted that the independent term of Eq. (4), whose value is 148 637 J mol^{-1}, is similar to other values found in the literature for the grain boundary self-diffusion energy of pure Fe$_\gamma$,[23,24] which is approximately equal to half of the lattice self-diffusion energy.[25–28] Thus, as the phenomenon which governs recrystallization is specially grain boundary self-diffusion, the absolute term in Eq. (4) is also a contribution to knowledge of the activation energy of this phenomenon. On the other hand, the different influence of the alloying elements on the value of Q has been explained elsewhere,[14] though perhaps it would be useful to remember that this influence

Table 5. Experimental values of experimental activation energy (Q_e), and calculated (Q_c) according to Eq. (4).

Steel	Q_e (Jmol^{-1})	Q_c (Jmol^{-1})
C1	159 000	165 386
C2	162 000	151 389
C3	148 000	137 398
S1	160 000	167 068
S2	245 000	243 961
M1	168 000	169 281
M3	190 000	187 683
Mo1	180 000	178 790
Mo2	193 000	192 774
Mo3	170 000	172 226
V1	177 000	180 358
V2	177 000	180 735
V3	182 000	181 464
V4	170 000	172 124
V5	171 000	168 485
V6	161 000	163 496
V7	168 000	165 767
V8	175 000	173 385
N1	252 000	248 299
N2	262 000	259 089
N3	230 000	229 286
N4	245 000	239 998
N5	198 000	214 949
N7	243 000	240 725
N8	222 000	218 860
N9	204 000	209 704

is probably due to the different strain that each element produces on the austenite. The greater the atomic volume of the substitutonial elements, the greater the distortion, and accordingly it should be remembered that the atomic volumes of the alloying elements keep the same relation of order as their influence on Q. The insterstitial element C lowers the activation energy, as the displacement of lattice atoms in the neighbourhood of a moving carbon atom would be larger than in the bulk of the crystal and vacancy diffusion occur preferentially in these circumstances.[30]

The values of Q calculated from Eq. (4) for all the steels have been set down in Table 5, and comparison of these values with the experimentally given values indicates good exactitude. A high correlation coefficient (0.99) between the experimental and calculated values was obtained (Fig. 7).

Though the influence of the Ti content was established in the old model,[14] it can be seen that the new expression (4) does not consider this influence, since it is very difficult to quantify. As was already considered in the first model, the influence of Ti on SRK is due both to the Ti in solution and the Ti that is precipitated at the austenitizing temperature, though it was not possible to distinguish between the contribution of these two states, and for this reason the influence of Ti was expressed in expression (4) as a function of the total percentage. However, recent studies have demonstrated that in addition to the total percentage of Ti, taken as a single variable in order to simplify the influence of this element on the value of Q, the distribution of the precipitates, *i.e.* the average precipitate size and the volume precipitated at the austenitizing temperature, are two other variables that influence the value of Q, and to express the influence of

both would be extremely complicated.[31)]

The nucleation of the new recrystallized grains preferentially takes place at the grain boundaries. For this reason the initial grain size will have an influence on recrystallization kinetics; the smaller the grain, the faster they become. According to Eq. (3), the value of 1.09, practically equal to one, was obtained for s.

On the other hand a value of -0.535 was obtained for q, and this confirms that the influence of strain rate on the recrystallized fraction is less than the influence of other variables (temperature, strain, grain size).

The values of p (Eq. (3)) were similar for all the steels, being between -1.48 and -2.32. Analysis of the variations of p suggests that it is influenced by the initial grain size (D), though most authors have opted for a constant value. However, the high number of readings obtained in this work allow us to make a reasonable valuation of p as a function of the initial grain size. The best relation found between p and D was of the type $p \propto D^{\alpha}$, similar to that found by other authors.[2)] The expression found for the regression curve of values of p against D for all the steels studied was as follows:

$$p = -4.3D^{-0.169} \quad \text{.....(5)}$$

Once the different parameters (Q, p, r, s) have been determined it only remains to determine coefficient A, so that $t_{0.5}$ may be calculated using Eq. (3). The value of A was determined for each steel by inserting into Eq. (3) the experimental values of $t_{0.5}$ and the corresponding temperature, strain and strain rate, as well as the values of the previously determined parameters. The values of A for each steel were very close, thus demonstrating that it is independent of the temperature, strain and strain rate. It was seen that there is a certain relation between A and Q predicted by Eq. (4) and that as the latter increases the former diminishes. Possible relations between both magnitudes were studied and it was found that the correlation of the exponential relation was very high, approximately 0.998, clearly demonstrating the dependence of A on the chemical composition, having found the following expression:

$$A = 3.754 \cdot 10^{-4} \exp(-7.869 \cdot 10^{-5} Q) \quad \text{.....(6)}$$

It should be noted that Eq. (6) shows a relation between A and Q which is similar to that found for other heat-activated physical phenomena and interpreted by means of an Arrhenius-type law.[30)] The values obtained for the exponent n of Eq. (2) showed a slight dependence on the temperature and were very similar for all the steels, the majority being between 0.56 and 1.4, depending on the temperature. Thus, two different expressions were found for low alloy (Eq. (7)) and microalloyed steels (Eq. (7)), respectively:

$$n = 2.93 \exp\left(-\frac{12\,500}{RT}\right) \quad \text{.....(7)}$$

$$n = 28.33 \exp\left(-\frac{36\,000}{RT}\right) \quad \text{.....(8)}$$

Once the expressions for $t_{0.5}$ and n were determined, SRK were modelled simply by inserting these expressions into Eq. (2).

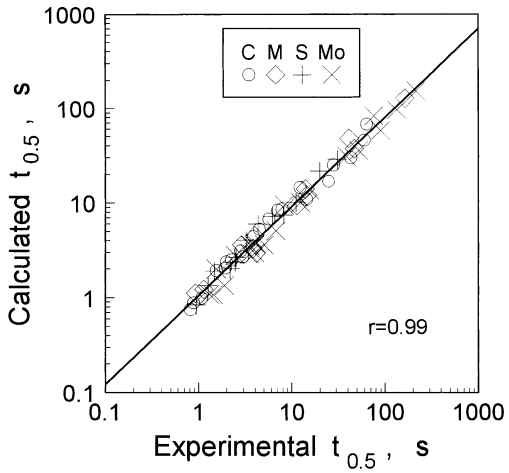

Fig. 8. Predicted $t_{0.5}$ according to Eq. (2) *vs.* experimental $t_{0.5}$ for low alloy steels. Steels C1, C2 and C3 are represented by C; M1 and M3 by M; S1 and S2 by S; Mo1, Mo2 and Mo3 by Mo.

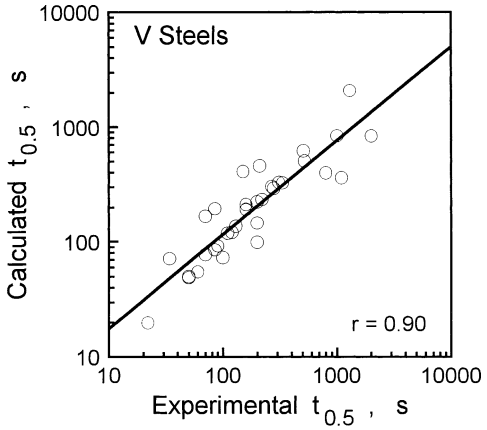

Fig. 9. Predicted $t_{0.5}$ according to Eq. (2) *vs.* experimental $t_{0.5}$ for V steels.

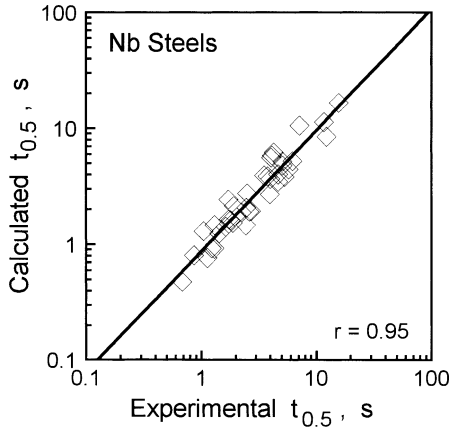

Fig. 10. Predicted $t_{0.5}$ according to Eq. (2) *vs.* experimental $t_{0.5}$ for Nb steels.

The model has been verified by comparing the experimentally determined recrystallized fraction curves with those predicted by Eq. (2). However, considering that $t_{0.5}$ is a more important parameter than n, since the latter varyies only a little from one steel to another and is only slightly dependent on the temperature, comparison between experimental $t_{0.5}$ and $t_{0.5}$ calculated using Eq. (3) for all the steels

Table 6. Parameter values of the old and improved models.

Parameters	Improved model	Old model [14,15]
Q ($Jmol^{-1}$)	148 636.8-71 981.3 (C%)+ 56 537.6 (Si%)+21 180 (Mn%)+ 121 243.3(Mo%)+64 469.6(V%)+ 109 731.9 $(Nb\%)^{0.15}$	124 714+ 64 716.7 (Si%)+ 28 385.7(Mn%)+72 775. 4(Mo%)+ 121 100.4$(Nb)^{0.1}$
p	$-4.3D^{-0.169}$	$-3.7D^{-0.137}$
q	-0.53	-0.53
s	1.09≈1	0.996≈1
A	$3.754x10^{-4}exp(-7.869x10^{-5}Q)$	$3.869x10^{-4}exp(-7.921x10^{-5}Q)$
N	2.93exp(-12 500/RT) 28.33exp(-36 000/RT)*	3.07exp(-12 000/RT) 38.02exp(-43 800/RT)*

*for Nb microalloyed steels

will be a good indicator of the model's predicting power and offers the material possibility of establishing a comparison for all the experimental values. In this respect the good prediction of the model has been verified, giving a correlation index of better than 0.92 for the twenty six-steels (**Figs. 8–10**).

In the case of microalloyed steels, it should be remembered that once induced precipitation has started, activation energy increases as a consequence of the rise in recrystallization inhibition energy. Though the X_a *versus* $\ln t$ curve once again comes to obey Avrami's law once the plateau has finalized, it has been verified that the new activation energy depends on the size and distribution of precipitates. Thus, to establish a model for recrystallization kinetics at temperatures below SRCT would require certain considerations and a specific treatment of the phenomenon.

Finally, **Table 6** shows the expressions and values of the different parameters in Eqs. (2) and (3), corresponding to the old and improved models, respectively, where it can be seen that the most important changes are due to the influence of V and C, which has been determined in the improved model proposed.

6. Conclusions

1. All the alloying elements have an influence on static recrystallization kinetics. The substititional elements increase the value of Q, especially Nb. In contrast, C, an interstitial element, contributes to lowering the value of Q.
2. The influence of grain size on static recrystallization kinetics is approximately linear.
3. The influence of strain on recrystallization kinetics is not independent of the microstructure, as it depends slightly on the grain size.
4. Exponent n in Avrami's equation diminishes slightly with the temperature.
5. Strain rate has less influence than strain and grain size, but its influence is not negligible.
6. The high correlation index ($r>0.92$) between experimental $t_{0.5}$ and calculated $t_{0.5}$ demonstrates the good prediction of the model.

Acknowledgements

The authors are grateful for the financial support of the CICYT of Spain. Quispe's studies were sponsored by the ICI (Spain).

REFERENCES

1) C. M. Sellars: Proc. Int. Conf. On Hot Working and Forming Processes, ed. by C. M Sellars and G. J. Davies, Met. Soc., London, (1980), 3.
2) P. Choquet, B. Lamberterie, C. Perdrix and H. Biausser: Proc. 4th Int. Steel Rolling Conf., ed. by IRSID, Deauville (France), (1987), B5.1.
3) C. M. Sellars: *Mater. Sci. Technol*., **6** (1990), 1072.
4) J. H. Beynon and C. M. Sellars: *ISIJ Int*., **32** (1992), 359.
5) T. Siwecki: *ISIJ Int*., **32** (1992), 368.
6) E. Anelli: *ISIJ Int*., **32** (1992), 440.
7) O. Kwon: *ISIJ Int.*, **32** (1992), 350.
8) A. Laarasoui and J. J. Jonas: *ISIJ Int*. **31** (1991), 95.
9) A. Laarasoui and J. J. Jonas: *Metall. Trans. A*, **22A** (1991), 151.
10) P. D. Hodgson and R. K. Gibbs: *ISIJ Int*., **32** (1992), 1329.
11) W. P. Sun, M. Militzer, E. B. Hawbolt and T. R. Meadowcroft: *Iron Steelmaker*, **12** (1998), 85.
12) S. Yamamoto, C. Ouchi and T. Osuka: Proc. Int. Conf. on Thermomechanical Processing of Microalloyed Austenite, ed. by A. J. De Ardo, G. A. Ratz and P. J. Wray, The Metallurgical Society of AIME, Pensylvania, (1982), 613.
13) J. J. Jonas and M. G. Akben: *Met. Forum*, **4** (1981), 92.
14) S. F. Medina and J. E. Mancilla: *ISIJ Int.*, **36** (1996), 1063.
15) S. F. Medina and J. E. Mancilla: *ISIJ Int.*, **36** (1996), 1070.
16) L. E. Toth and A. W. Searcy: *Trans. Metall Soc. AIME*, **230** (1964), 690.
17) E. T. Turkdogan: *Iron Steelmaker*, **3** (1989), 61.
18) A. Faessel: *Rev. Métall.*, *Cah. Inf. Tech*., **33** (1976), 875.
19) H. L. Andrade, M. G. Akben and J. J. Jonas: *Metall. Trans. A*., **14A** (1983), 1967.
20) J. S. Perttula and L. P. Karjalainem: *Mater. Sci. Technol*., **14** (1998), 626.
21) P. Choquet, A. Le Bon and C. Perdrix: Proc. Int. Conf. on Strength of Metals and Alloys, CISMA 7, Vol. 3, ed. by H. J. Mcqueen, J. B. Bailon, J. I. Dickson, J. J. Jonas and M. G. Akben, Pergamon Press, Oxford, (1986), 1205.
22) S. F. Medina, A. Quispe and M. Gómez: *Mater. Sci. Technol*., **17** (2001), 536.
23) Y. Adda and J. Philibert: La Difussion dans les Solides, Institut National des Sciences et Techniques Nucléaires, Vol. 2, Saclay, France, (1966), 718.
24) A. Rosen, M. S. Burton and G. V. Smith: *Trans. AIME*, **230** (1964), 205.
25) F. S. Buffington, K. Hirano and M. Cohen: *Acta Metall*., **9** (1961), 434.
26) W. S. Young and H. Mikura: *Acta Metall*., **13** (1965), 449.
27) H. W. Mead and C. E Birchenall: *J. Met. Trans. AIME*, **208** (1956), 1336.
28) B. Sparke, D. W. James and G. M. J. Leak: *Iron Steel Inst*., **203** (1965), 152.
29) H. W. Mead and C. E. Birchenall: *J. Met. Trans. AIME*, **204** (1956), 1336.
30) S. F. Medina and C. A. Hernández: *Acta Mater*, **44** (1996), 137.
31) S. F. Medina, M. I. Vega and A. Quispe: *Steel Res.*, **72** (2001), 24.